Journal of Crystal Growth 61 (1983) 556–566
North-Holland Publishing Company

MODIFIED WULFF CONSTRUCTIONS FOR TWINNED PARTICLES

L.D. MARKS

Department of Physics, University of Cambridge, Madingley Road, Cambridge CB3 0HE, UK

Received 2 July 1982; manuscript received in final form 14 September 1982

This paper reports the application of a modified form of the Wulff construction to derive theoretical shapes and total surface energies for twinned particles. It is proposed that the incorporation of twin boundaries in faceted particles leads to a number of constrained local minimum in the total surface energy (at constant volume), in addition to the minimum of a single crystal Wulff polyhedron. A procedure for generating these constrained local minima is described. The model is then applied to determine the structures of twinned particles in face-centred materials. Two possible configurations are examined, an arrangement where the crystals are symmetric about the twin boundaries, and an asymmetric configuration. Shapes and total surface energies for a large number of twinned structures are given using a simple model which includes only (111) and (100) surface facets. Excellent agreement is obtained between the theoretical model and experimental results.

1. Introduction

A detailed understanding of the morphologies of small particles is an important problem in a number of fields. The thermodynamic processes for single crystals are well understood through the Wulff construction [1], but the more general problem of polycrystals or twinned particles is not. In a recent paper [2], a model was proposed based upon a modified form of the Wulff construction and successfully applied to the surface morphology of multiply twinned particles or MTPs. (The basic sources for structural details on MTPs are the original papers by Ino [3], and Ino and Ogawa [4]). In particular, the model accounted for the experimental observation of re-entrant surfaces at the twin boundaries of annealed decahedral MTPs. These re-entrant surfaces are not due to any twin boundary grooving effect, but instead are thermodynamic features which significantly lower the total surface energy of the particles leading to an approximately spherical shape.

In this paper a modified form of the Wulff construction is applied to the general problem of the surface morphologies of twinned particles. It is proposed that in faceted particles a qualitative breakdown of the liquid-like model for small particles [5–7] occurs, and local constrained minima arise from the restricting effect of the twin boundaries. Excellent agreement is obtained with experimental evidence for twins in small face-centred cubic particles.

2. The modified Wulff construction

The problem which is dealt with in this section is a minimisation at constant volume of the total surface and twin boundary energy in a particle. A condition for a possible local constrained minimum of these energy terms is described. The basis for this analysis is the Wulff construction [1], which is used here to substantially reduce the number of variables in the problem. Given a form for the surface free energy $\gamma_S(\theta,\phi)$ as a function of the normal direction in spherical polar coordinates, θ,ϕ, the construction takes the form: (1) construct the surface $\boldsymbol{r} = \gamma_S(\theta,\phi)\hat{r}$, (2) draw the planes normal to this surface at all points, and (3) take the inner envelope of these planes.

The construction is illustrated in two dimensions in fig. 1. Proofs of the construction have been presented by Laue [8] and Dinghas [9].

In order to employ this construction to de-

0022-0248/83/0000–0000/$03.00

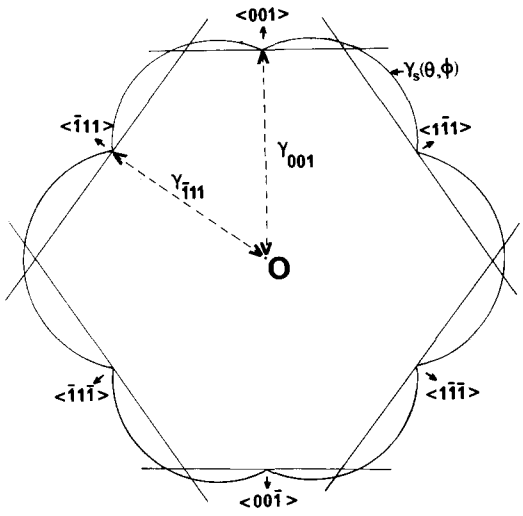

Fig. 1. An example of a two-dimensional Wulff construction for an fcc material on a (110) plane. The form of $\gamma_S(\theta,\phi)$ used would lead to a strong faceting model.

termine the equilibrium morphologies of twinned particles, consider first the simple structure of a particle with only one twin boundary; the arguments that apply to this structure can be readily extended to more complicated twinned particles. We begin by partitioning the energy per unit area of the twin boundary (γ_t) into two parts, associating $\alpha\gamma_t$ with single crystal element A and $(1-\alpha)\gamma_t$ with element B (where α is for the moment arbitrary). We now cut the particle down the twin boundary and nominally separate the two components A and B. This operation allows us to consider the twin faces on A and B as external surface facets or "twin facets" of energy per unit area $\alpha\gamma_t$ and $(1-\alpha)\gamma_t$ respectively. We can now solve for the minimum surface energy configuration of A and B taken independently by using a Wulff construction in which the twin boundary facets are represented by extra point values of $\alpha\gamma_t$ or $(1-\alpha)\gamma_t$ in the original $\gamma_S(\theta,\phi)$ surface energy function. Any local minimum of the complete particle must also be a local minimum for the two sections A and B taken independently. Hence by partitioning the particle as described above we have reduced the number of variables in the problem to α and the relative volumes of A and B; the problem is already minimised as far as the arrangement of the external surface facets is concerned.

The two components A and B must now be joined together to complete the particle and the minimisation problem. This introduces an important constraint – the two twin facets must be identical. The strength and the nature of this constraint is critically dependent upon the form of $\gamma_S(\theta,\phi)$. For example, the constraint has no appreciable effect for the two simplest and most convenient models of $\gamma_S(\theta,\phi)$, a liquid-like model [5–7] where the Wulff polyhedron is a sphere, or any two-dimensional representation. For both of these, with a given value of the partition α the twin facets can be matched with an appropriate value of the relative volumes. Here the constraint reduces the number of free variables to just one, the partition α which can take a continuous range of values. The effect of variations using this remaining degree of freedom must now be considered. Since the twin boundary contributes a detrimental term to the total energy of the particle, it will preferentially migrate out of the particle. (This corresponds to letting α tend towards plus or minus infinity.) Here the only minima are when either A or B vanishes.

In contrast, for an arbitrary form of $\gamma_S(\theta,\phi)$ or one with only the limited symmetry of the crystal point group, the constraint has a totally different effect. For an arbitrary value of α it is impossible to match the twin facets, however we vary the

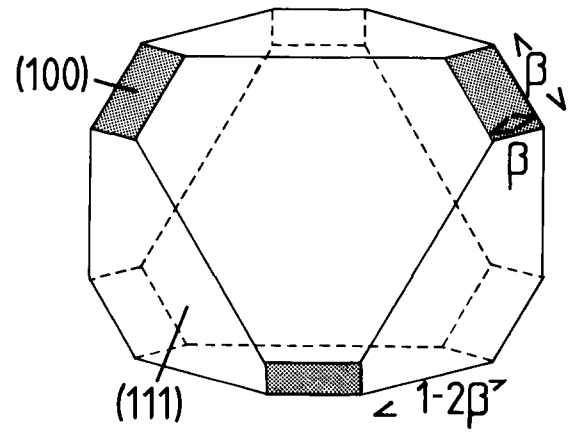

Fig. 2. The shape of a single crystal in a Strong Faceting model, with $\beta = 1 - \gamma_{100}/\sqrt{3}\,\gamma_{111}$.

Table 1

Particle	ϵ_ω^3		ϵ_ω	
			$\beta = 1/3$, $\eta = 0.005$	$\beta = 5/12$, $\eta = 0.005$
Single crystal	$108\sqrt{3}(1-3\beta^3)$		5.499	5.271
LTP with m twin boundaries	$108\sqrt{3}\{1-3\beta^3+\frac{3}{8}\eta m[5+2\eta(1-\eta)]\}$	$m=1$	5.500	5.272
		$m=2$	5.500	5.273
		$m=3$	5.501	5.274
		$m=4$	5.502	5.275
Decahedral MTP	$\frac{101}{4}\sqrt{3}[(1+\eta)^3-\frac{8}{3}(\beta^3+\eta^3)]$		5.436	5.243
Icosahedral MTP	$\frac{67}{2}\sqrt{3}[(1+3\eta)^3-24\eta^3]$		4.899	4.899
Bi-icosahedral MTP	$\frac{67}{2}\sqrt{3}(\frac{216}{196})(1+11\eta)$		5.051	5.051
Asymmetric twin	$108\sqrt{3}\{1-3\beta^3+\frac{1}{2}S\eta[\frac{1}{4}\beta\eta+(1-2\beta)(2-3\beta)]\}$		–	5.272
Asymmetric decahedral MTP	$108\sqrt{3}\{1-3\beta^3+\frac{1}{4}(\frac{1}{4}-\beta^2)-(1-\beta)(3\beta-1)^2+\frac{3}{8}\eta[5+\beta(1+\beta)]\}$		–	5.256

Formulae and numerical values for the particles considered herein. For simplicity, ϵ_ω values for the bi-icosahedral MTP and the asymmetric Dh have been evaluated by a perturbation technique [2], where γ_t is set to zero and the twin boundary contribution is derived from the appropriate boundary area. (This is accurate to first order.) The notation used is $\beta = 1-\gamma_{100}/\sqrt{3}\,\gamma_{111}$, $\eta = \gamma_t/2\gamma_{111}$ and $S = (1+n^2/4\beta^2)^{1/2} - \eta/2\beta$, where γ_{111}, γ_{100} and γ_t are the energies per unit area of, respectively, (111), (100) faces and a twin boundary. The asymmetic twins are valid for $1/3 \leqslant \beta \leqslant 1/2$, all others for $0 \leqslant \beta \leqslant 1/2$.

relative volumes. This is because there is only a limited symmetry to the Wulff polyhedron, e.g. the shape for an fcc material with only (111) and (100) facets (hereafter referred to as a Strong Faceting model) * as shown in fig. 2. The constraint can only be satisfied for a small number of discrete values of α and the relative volumes of A and B, and not for a continuous range of values. (In practice, the only way to verify this for the twin plane of interest is to construct the appropriate twin facets and then check, by trial and error, whether discrete values only or a continuous range exists. Exceptional cases will arise when a continuous range is possible, but as a *general* rule, only discrete values will be possible.) There is a minimum for an untwinned single crystal, i.e. when either A or B vanishes, and there may also be constrained local minima for any or all the other discrete values where the constraint is satisfied. The degree of freedom that was present in both the liquid-like model and the two-dimensional representation (when α was a continuous free variable) is no longer present. At any of these discrete points the only way in which the twin boundary can migrate out of the particle is when the outer surface also deforms. This can be seen from the structure of an fcc particle with one twin boundary which is shown for a Strong Faceting model in fig. 3. A twin boundary energy (per unit area) is in general only a few percent of a typical surface energy for the external faces. Therefore the additional deformation of the external surface may require more energy than can be obtained by reducing the total twin boundary area. Hence the constraint of the twin boundary which couples migration of the twin boundary with deformations of the outer surface may force local minima which would not otherwise occur.

It is useful to visualise the configuraion at one of these constrained local minima with a potential energy surface as shown in fig. 4. The local minimum is situated in a valley with very steep sides,

* The parameter $\beta = 1-\gamma 100/\sqrt{3}\,\gamma_{111}$ will be employed throughout this paper to describe the significance of the (100) facet surface energy (γ_{100}) relative to the (111) facet surface energy (γ_{111}), being used both in the context of a relative length in the figures and as a dimensionless constant in the energy calculations (table 1).

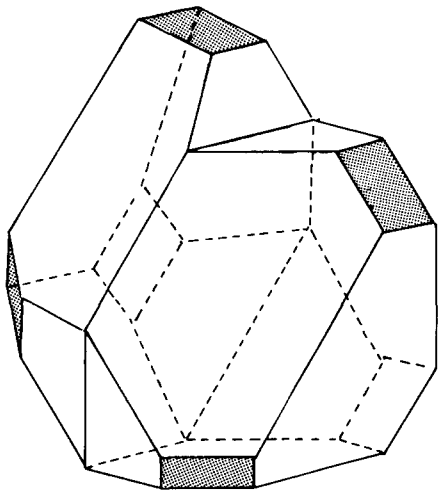

Fig. 3. The shape of a single crystal with one twin boundary drawn for a partition $\alpha = 1/2$ and the same volume in the two segments. The (100) faces are shaded.

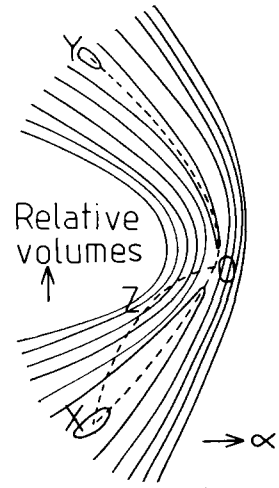

Fig. 4. Diagram to illustrate the potential energy surface for a twinned particle. Energy contours corresponding to non-equilibrium values of the relative volumes and the parameter α are shown, all the other variables (i.e. the external surfaces) being minimised. The particle would like to descend down the valley floors OX or OY, but is prescribed by the geometry of the twin to move along OZX, which would involve climbing the valley sides. Here X and Y describe the positions of single crystals, and O one of the constrained minima (a modified Wulff construction).

these sides representing deformations of the outer surface. There is a gentle slope along the floor of the valley which represents migration of the twin boundary. With a liquid model or a two-dimensional representation the constraint is weak and the twin boundary can migrate along the valley floor. In contrast, in a Strong Faceting model the constraint couples motion of the twin boundary and the external surface by restricting the possible paths the particle can move on (as illustrated in fig. 4). This requires the particle to climb up the steep sides of the valleys when the twin boundary migrates, which can be an uphill route. To what extent this is uphill will depend in a complicated fashion upon the exact form of $\gamma_S(\theta,\phi)$.

The analysis described above can be extended to deal with an paricle containing an arbitrary number of twin boundaries. As before, we divide up the twin boundaries and minimise the separate single crystal components individually using a Wulff construction into which we introduce twin facets. In general there will be only a limited number of discrete values for partitions of the twin boundaries and the relative volumes of the different single crystal elements for which the various segments will fit together. Each of thse configurations is a possible constrained local minimum.

We therefore propose the following model for possible constrained local minima in the energy of twinned particles:

(1) Construct a Wulff polyhedron as per the standard Wulff construction.

(2) Extract the appropriate area by including the twin boundaries in the equivalent form of external twin facets of energy per unit area $\alpha\gamma_t$ and $(1-\alpha)\gamma_t$.

(3) Find any discrete values of α and the relative volumes for which the twin facets can be matched. If there is a continuous range of values, no constrained minima exist.

This solution for possible local minima will be termed a modified Wulff construction. There will always be one possible solution, a symmetric arrangement where $\alpha = \frac{1}{2}$ and the volumes are equal. An example of this symmetric construction for a decahedral MTP is shown in fig. 5. This is true for any crystallography and is forced by the reflection symmetry of a twin boundary. This solution has been previously employed for multiply twinned particles [2] where an equal partition was invoked from the known symmetry of the par-

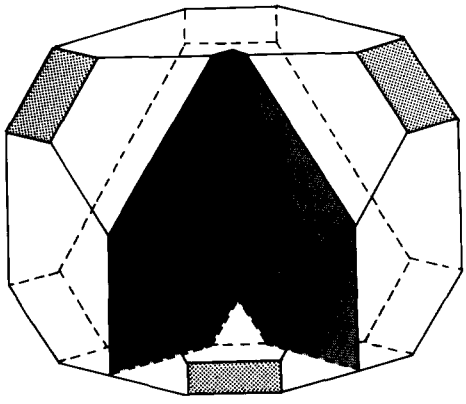

Fig. 5. A symmetric, modified Wulff construction for a decahedral MTP. In this case we extract the region between two twin facets on inclined (111) planes (shaded) from the single crystal Wulff polyhedron.

ticles. The results for MTPs strongly reinforce the hypothesis of a constrained local minimum: for many forms of the surface faceting direct numerical evaluation shows that MTPs have lower surface energies than single crystals of the same volume, and are therefore not just constrained local minima but full unconstrained local or even global minima. For the particular case of a fcc material and a Strong Faceting model there is a second solution where the partition is asymmetrical, as described below. Both the symmetric and asymmetric solutions are in good agreement with experimental particle structures.

3. Applications of the symmetric twin to fcc materials

3.1. Lamellar twinned particles

The simplest particles where the model can be used have a number of parallel twin boundaries, and are called lamellar-twinned particles or LTPs. When produced in argon smokes [10], LTPs are characterised by:

(1) closely packed twin boundaries near the middle of the particles;

(2) particles with an odd number of boundaries resembling two halves of a single crystal reflected about the central, twinned region;

(3) particles with an even number of boundaries resembling single crystals.

All LTPs can be constructed from two building blocks, a single crystal with one twin facet and a crystal with two twin facets. The components are shown in fig. 6 for a Strong Faceting model. To generate LTPs we sandwich a number of the plates with two twin facets between a pair of the larger components which have one twin facet, suitably reflecting these elements at the twin boundaries. The structure of the first two members, a particle with one twin boundary and a particle with two are shown in figs. 3 and 7 respectively. As γ_t is small compared to a surface energy, the twin boundaries are closely spaced near the centre of the particles and the twin faces are appproximately hexagons. All the generalisations quoted

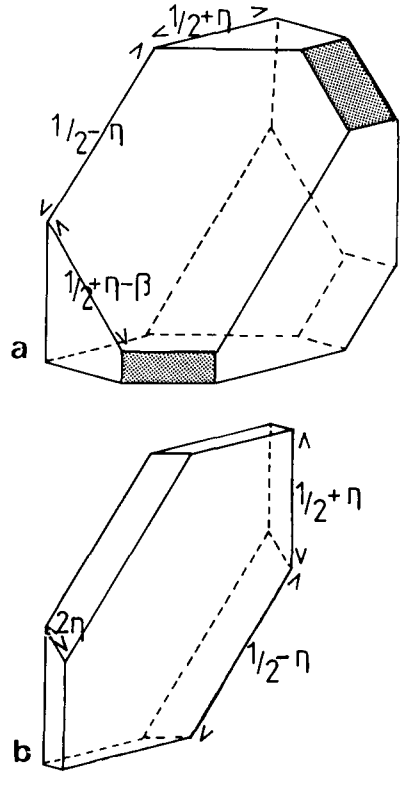

Fig. 6. The components for generating LTPs: (a) a segment with one twin facet and (b) the thin plate with two twin facets. The magnitude of γ_t has been exaggerated for clarity. The (100) facets are shaded.

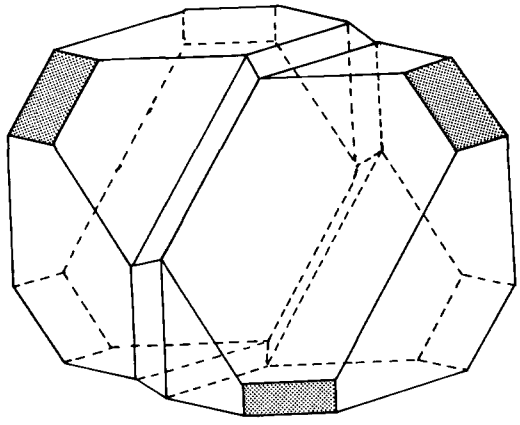

Fig. 7. The structure of an LTP with two twin boundaries. The central plate region will tend towards a stacking fault in a small particle. The (100) facets are shaded.

above are reproduced by the model.

One particular feature of LTPs should be noted: the presence of three large re-entrant surfaces or notches on the particles with an odd number of twin boundaries. These features are not due to any form of twin boundary grooving. (Twin boundary effects are present in the particles, but are so small as to be practically undetectable. They can be removed by setting the twin boundary energy equal to zero, which causes structural modifications of the order of $\gamma_t/2\gamma_S(\theta,\phi)$, i.e. 1 or 2% at most.) These notches arise simply from the reflection symmetry of the twin boundaries.

Similar structures (primarily particles with only one twin boundary) have also been observed in annealed gold particles on an amorphous carbon film [11], platinum model catalysts [12], silver model catalysts [13] and evaporated gold and silver particles [14]. The dominance of the mono-twin is probably because in very small particles the equilibrium intertwin separation predicted by the construction will be only a few atomic layers. It will then be energetically favourable for pairs of twin boundaries to collapse to a stacking fault and be eliminated by the passage of a partial dislocation.

The surface energy contribution to the free energy of a Wulff construction can be conveniently represented by a dimensionless parameter ϵ_ω given by

$$\epsilon_\omega = \frac{\int \gamma_S(\theta,\phi)\, dS}{\gamma_{111} V^{2/3}},$$

so that

$$G_{\text{surface}} = \epsilon_\omega \gamma_{111} V^{2/3},$$

where γ_{111} is the surface energy per unit area of a (111) face and V is the particle volume. Values for ϵ_ω for LTPs and the other structures considered herein are given in table 1 (for a Stong Faceting model).

3.2. Multiply-twinned particles

The use of the model for multiply-twinned particles (MTPs) has been dealt with in detail elsewhere [2]. They are included here to stress their relationship to the other twinned structures – in MTPs the twin boundaries are not parallel but occur in inclined (111) planes. Five single crystal units, with two boundaries each, assemble to a decahedral MTP of Dh, whilst an icosahedral MTP

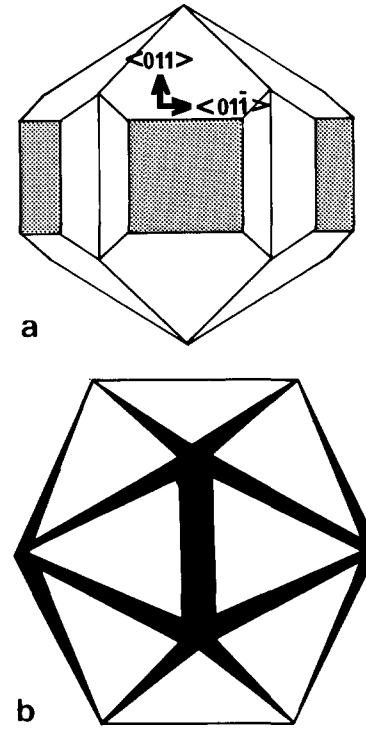

Fig. 8. The structure of MTPs in a strong faceting model: (a) a Dh (front surface only) drawn for $\beta = 1/3$ and (b) an Ic which is here an icosahedron. Very small additional facets from twin boundary grooving [2] are present, but have disappeared in the drafting. As before, the (100) facets are shaded.

has 20 units with three twin boundaries each. As such, neither MTP is completely space filling and it is necessary to incorporate a small internal distortion in the form of either an inhomogeneous strain or dislocations. (A more detailed analysis of this internal deformation will be given elsewhere [15].) The structures of the two particles are shown for reference in fig. 8. As for the LTPs described above, the symmetric partition is a configuration where the units fit together (and, for the same geometric reason, there are re-entrant surfaces at the twin boundaries of the Dhs). Explicit evaluation (ref. [2] and table 1) shows that for many forms of $\gamma_S(\theta,\phi)$ the symmetric partition for MTPs is a true minimum with a smaller total surface energy than a single crystal. (However, the surface energy alone does not determine whether MTPs or single crystals are the preferred form for any volume. There is an additional, detrimental elastic strain energy in MTPs from the internal distortion mentioned above. A more detailed analysis of these elastic terms and the energy balance between MTPs and single crystals will be given elsewhere [15].)

3.3. Polyparticles

In the early stages of particulate growth, forms occur which resemble polycrystals, except that instead of being built from single crystals, whole particles such as LTPs or MTPs are involved [14]. One of the more common of these "polyparticles" is the bi-icosahedral MTP which is composed of two Ics sharing five tetrahedral units. To analyse this particle, consider 35 segments with 3 twin facets each and 5 with 4 twin facets. Due to the constraint action of the twin boundaries, the size of the segments with four twin facets is completely prescribed by the neighbouring segments. Assuming next a strong faceting model for $\gamma_S(\theta,\phi)$, the shape of the remaining segments is a tetrahedron with three vanishingly small extra facets from the twin boundary grooving effect [2]. Ignoring the very small facets for clarity (as this has no appreciable effect upon the structure), the shape for the assembled structure is shown in fig. 9. This is in excellent agreement with the structure reported by Smith and Marks [14]. However, many polyparticles cannot be fitted with a symmetric partition, for example, a decahedral–icosahedral MTP where two tetrehedral segments are shared. It may be that a more complicated asymmetric partition is involved, or alternatively the particles may be frozen in an intermediary stage of coalescence. (Partially coalesced particles, e.g. single crystals in the necking stage of coalescence, were observed in the same sample [14].) Further work, in particular

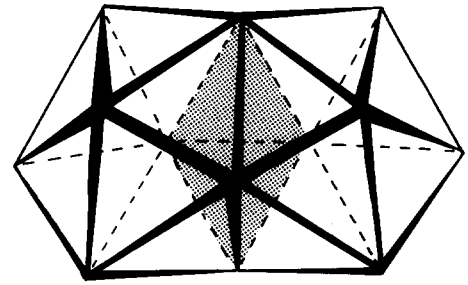

Fig. 9. The shape of a bi-icosahedral MTP. The five shaded segments are shared.

Fig. 10. A high resolution lattice image showing a Dh embedded in a two-dimensional polyparticle network. This can be compared with the lattice images given by Marks and Smith [19].

in-situ observations during annealing, would be of interest.

The polyparticle model can be extended to rather large numbers of particles when it is equivalent to a polytetrahedral model [16–18]. Preliminary results suggest that a two-dimensional form of this extended polyparticle model does occur for room temperature growth of gold on rocksalt. Fig. 10 shows such an area in a film grown in 5×10^{-6} Torr of oxygen.

4. Asymmetric twinning for fcc materials

The conditions used in section 2 to describe a possible local minimum were external facets in the arrangement of a Wulff construction, a partition α and $1-\alpha$ of the twin boundary such that the twin facets matched, and insufficient symmetry in the structure for the twin boundary to migrate out. In general the symmetric modified Wulff construction with $\alpha = \frac{1}{2}$ need not be the only solution for a constrained minimum. With a Strong Faceting model a second, asymmetric solution also exists as illustrated in fig. 11. Similar to the symmetric twinning in LTPs, the twin plane here has a shape very similar to a hexagon. (The presence of three, sightly re-entrant surfaces at the twin boundary should be noted. These features can be used to identify this form of twinning.)

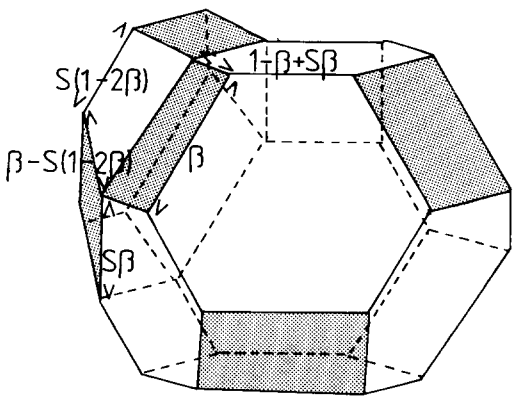

Fig. 11. The form of an asymmetric twin in an fcc material with a Strong Faceting model; (100) facets are shaded.

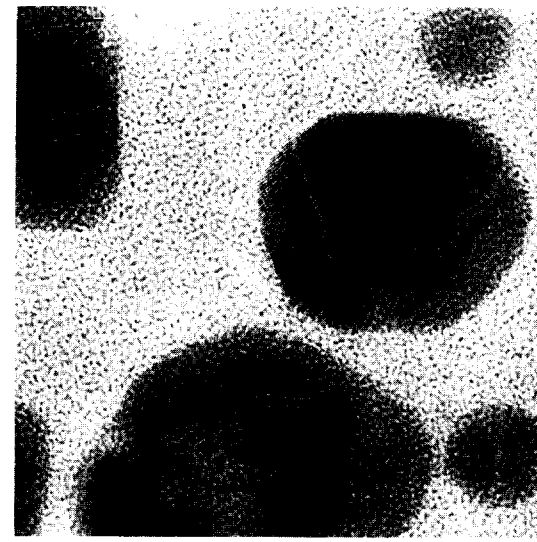

Fig. 12. A high resolution lattice image of an asymmetric twin. Details of the experimental procedure have been given elsewhere [14,19].

This structure corresponds to a partition with

$$\alpha = \tfrac{3}{2} - 2\beta + S\beta,$$

where the smaller segment is contracted by a factor

$$S = \left(1 + \eta^2/4\beta^2\right)^{1/2} - \eta/2$$

relative to the larger segment to fit at the twin boundary. This type of particle can only exist if the edge along which a (100) facet meets a (111) facet is longer than the edge where two (111) facets meet. This will occur if the ratio of the surface energy of a (111) facet to that of a (100) facet is greater than $\sqrt{3}/2$. (For a broken bond model the ratio is exactly $\sqrt{3}/2$.) Despite the oversimplifications of the zero faceting model, this second, asymmetric solution frequently occurs in fcc materials. A typical example is shown in fig. 12. Similar structures have also been observed in annealed gold particles on an amorphous carbon support [11].

The asymmetric cut can also be applied to particles with intersecting twin boundaries such as MTPs. For example, in a Dh a second form can be

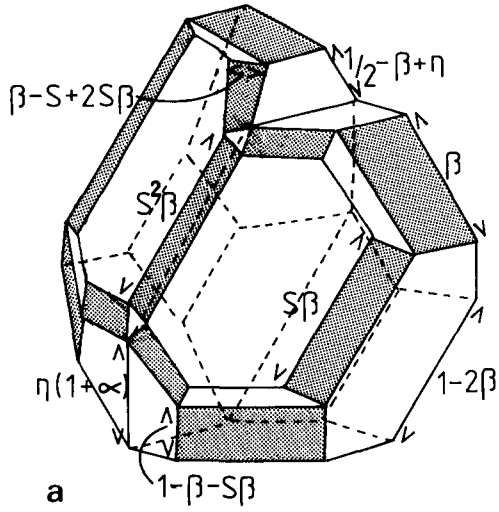

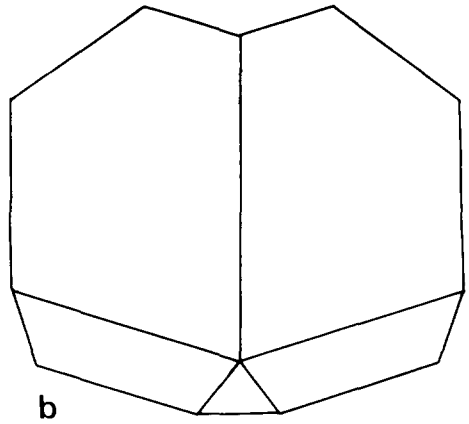

Fig. 13. The structure of an asymmetric Dh. In (a) the full three-dimensional shape is shown with the (100) facets shaded, whilst (b) is a (110) section which can be compared with the particle in fig. 15.

constructed with a strong faceting model where the five segments meet well away from the centre of the particle, as shown in fig. 13. This structure can be derived from the particle with one twin boundary shown previously in fig. 3. Two asymmetric twins are placed to one side of fig. 3, as illustrated in fig. 14. The fifth, smallest segments fits in between the two, having an asymmetric twin relationship to both of the thin segments. A small angular gap remains (as in the symmetric Dhs) which will be filled by inhomogeneous strain or a grain boundary. This configuration occurs in practice, as for example in the particle shown in fig. 15.

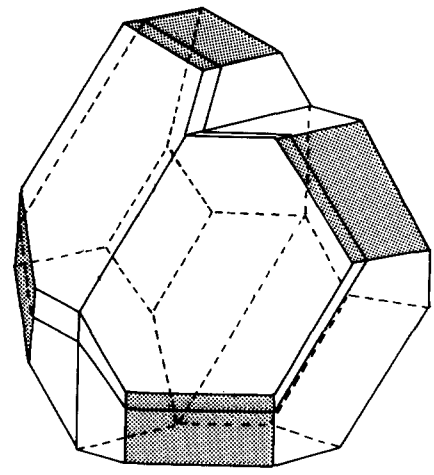

Fig. 14. Diagram to illustrate the generation of an asymmetric Dh from a particle with one twin boundary. The location of the asymmetric cuts are indicated. The (100) facets are shaded.

An important report of an asymmetric Dh was during in-situ growth of MTPs [22]. The process observed was the transformation of a particle with

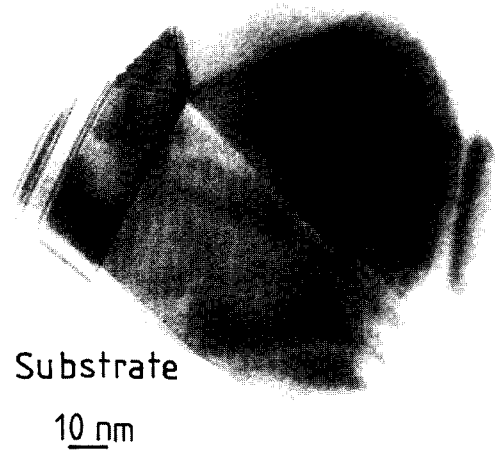

Fig. 15. A large, asymmetric Dh from a silver catalyst sample [20]. The specimen was similar to one reported upon elsewhere [21]. The particle is sitting on an α-alumina substrate in the region indicated, and there is some extra, twinned material to one side. The presence of microtwins in the smallest segment should be noted, which presumably terminate in dislocations thereby forming a grain boundary.

one twin boundary to an asymmetric twin and then to a symmetric Dh. Employing the potential energy surface formalism for small particles as described in section 2, deformation of a symmetric Dh to an asymmetric Dh and then to a particle with one twin boundary corresponds to motion along the floor of the valley and migration of the twin boundaries out of the structure. However, direct evaluation shows that (with a Strong Faceting model as in table 1) the total surface energy term will tend to drive the twin boundaries in, corresponding to the experimental observations. This agreement between the theoretical predictions of this paper and the experimental observations, in particular the observation of an asymmetric Dh as an intermediary, provides direct evidence for the existence of local constrained minima for twinned structures.

5. Discussion

The success of the modified Wulff construction in modelling the structure of many complicated twinned particles is encouraging. The hypothesis that modified Wulff constructions correspond to constrained local minima appears to be well substantiated by experimental evidence. Although the model explains the structures of a large number of twinned particles, on its own it does not account for the profusion of particle morphologies commonly observed (see, for example, ref. [14]). Many of the standard shapes, e.g. tetrahedra with (111) facets, can probably be attributed to kinetic effects in the early stages of growth.

In principle the model can be used with any crystallography and need not be restricted to simple twin boundaries or an fcc material. For example, higher order twin boundaries can be deal with simply by changing the direction and magnitude of the twin facets. Furthermore, the model is independent of the exact form of the Wulff construction. The precise form of the external surfaces and the total surface energies will vary with $\gamma_S(\theta,\phi)$, but the general results do not. However, the existence of the local minima will depend upon the form of the faceting. As the faceting becomes more isotropic (e.g. at higher temperatures), the restraint action of the twin boundaries is lifted and the minima convert to saddle points. An area of some interest for small particles is an understanding of the conditions when this "phase change" in the twinning occurs. Further experimental and theoretical work, for example investigations of both the shapes and the relative concentrations of particle types as a function of temperature, would be of considerable interest. An improved, mathematical model for examining the local minima would also be invaluable. However, the problem is deceptively simple. It is possible to show that the symmetric modified Wulff construction satisfies the conditions for a stationary point using the approach of Laue [8], but obtaining the sign of the second derivative is intractable. It is possible that a numerical evaluation would be easier than an analytic approach. At present the proof of the construction is the agreement achieved with experimental structures.

Acknowledgements

The author is indebted to Drs. A. Howie and D.J. Smith for their advice and the SRC for financial support.

References

[1] G. Wulff, Z. Krist. 34 (1901) 449.
[2] L.D. Marks, Phil. Mag., in press.
[3] S. Ino, J. Phys. Soc. Japan 21 (1966) 346.
[4] S. Ino and T. Ogawa, J. Phys. Soc. Japan 22 (1967) 1369.
[5] D.W. Pashley, M.J. Stowell, M.H. Jacobs and T.J. Law, Phil. Mag. 10 (1964) 103, 127.
[6] M.H. Jacobs, D.W. Pashley and M.J. Stowell, Phil. Mag. 13 (1966) 121,129.
[7] D.W. Pashley and M.J. Stowell, J. Vacuum Sci. Technol. 3 (1966) 156.
[8] M. von Laue, Z. Krist. 105 (1943) 124.
[9] A. Dinghas, Z. Krist. 105 (1943) 305.
[10] T. Hayashi, T. Ohno, Y. Shigeki and R. Uyeda, Japan. J. Appl. Phys. 16 (1977) 705.
[11] I. Hansson and A. Tholen, Phil. Mag. 37 (1978) 535.
[12] D. White, private communication.
[13] T. Cunningham, private communication.
[14] D.J. Smith and L.D. Marks, J. Crystal Growth 54 (1981) 433.
[15] A. Howie, L.D. Marks and E. Yoffe, in preparation.

[16] M.R. Hoare and P. Pal, J. Crystal Growth 17 (1972) 77.
[17] P.H. Gaskell, Phil. Mag. 32 (1975) 211.
[18] P.H. Gaskell and A.B. Mistry, Phil. Mag. A39 (1979) 245.
[19] L.D. Marks and D.J. Smith, J. Crystal Growth 54 (1981) 433.
[20] D. Wheatly, private communication.
[21] L.D. Marks and A. Howie, Nature 282 (1979) 196.
[22] K. Yagi, K. Takayamagi, K. Kobayashi and G. Honjo, J Crystal Growth 28 (1975) 117.